Science & Technology Development Journal – Engineering and Technology 2023, 5(SI2): 65-76

Open Access Full Text Article

Research article

Influence of temperature and porosities on free vibration of a three-phase bidirectional functionally graded sandwich beam

Pham Thi Ba Lien, Vu Thi An Ninh*

ABSTRACT

Understanding the influence of practical factors on natural frequencies of beams play an important role in design of this structure. This article explores the influence of temperature and porosities on vibration characteristics of a sandwich beam made from a three-phase bidirectional functionally graded material (BFGSW beam) for the first time. The sandwich beam composed from a homogeneous core and two face layers made of a three-phase composite material. The material properties are graded in both the beam axis and thickness by power-law functions, and they are evaluated by using the Voigt model. Heat loading with uniform temperature rise and even distribution of porosities are also considered. The expressions of the elastic strain energy and the kinetic energy for the beam as well as the strain energy due to temperature are obtained in the framework of the hyperbolic shear deformation theory. A two-node beam element with eight degrees of freedom has been proposed and used to establish the discretized equation of motion for the beam. The proposed method is validated by comparing the fundamental frequency parameters with two previous works. The beam with simply supported ends are used in numerical studies. The convergence of the derived beam element is represented by evaluating the fundamental frequency parameters. The effects of the temperature rise, the porosity volume fraction, the material indexes, the length to height ratio as well as the beam layer thickness ratio on the vibration characteristics are investigated and discussed in detail. It is concluded that the BFGSW beam parameters, the temperature rise and porous parameter play an important role in the natural frequency, which is helpful for the design of beam – like structures with the desired natural frequency.

Key words: Three-phase BFGSW beam, hyperbolic theory, porosity, natural frequency, finite element analysis

University of Transport and Communications, No 3 Cau Giay Street, Hanoi, Vietnam

Correspondence

Vu Thi An Ninh, University of Transport and Communications, No 3 Cau Giay Street, Hanoi, Vietnam

Email: vuthianninh@utc.edu.vn

History

- Received: 20-4-2023
- Accepted: 12-9-2023
- Published Online: 31-12-2023

DOI :

https://doi.org/10.32508/stdjet.v6iSI2.1095

INTRODUCTION

The functionally graded materials (FGMs) with continuously variable material properties in one or more spatial directions are considered as an advanced type of composites. FGMs are usually made from ceramics and metals, and it inherits the characteristic properties of the constituent materials such as the good heat resistance of ceramics and the high toughness of metals. Thanks to the attractive properties, FGMs gain wide applications in a high-temperature environment as automobile engines, nuclear reactors, rockets, etc [1]. The effects of temperature on natural frequencies of FGM beams [2–4], and functionally graded sandwich (FGSW) beam [5–7] have been reported.

Because of the large difference in the solidification temperature between the constituent materials during the FGM manufacturing process, porosities are often formed in FGMs during fabrication process. Vibration investigations of FGM beams taking the influence of porosities into consideration have drawn much attention from researchers in recent years. Wattanasakulpong and Ungbhakorn [8] investigated linear and nonlinear free vibrations of porous FGM beams in the framework of the classical beam theory and the modified rule of mixture. Using Navier solution, Ait Atmane et al. [9] investigated the free vibration, bending and buckling behavior of FGM beams resting on a two-parameter elastic foundation, considering the porosity effect. Several authors reported the impact role of porosities on vibration of FGM beams in temperature environment using different methods; the finite element method [10], Euler-Bernoulli beam theory combined with Navier solution method [11], the analytical method based on four-variable theory [12]. It has been shown that both the porosities and temperature significantly alter the vibration frequencies of FGM beams. Liu et al. [13] adopted the high-order trigonometric shear deformation theory to study the thermal-mechanical coupling buckling behavior of a porous FGSW beam clamped at both ends. The sandwich beam of the work is two-phase composite, and it is constructed from a FGM core and two face sheets of an isotropic homogeneous material.

Cite this article : Lien P T B, Ninh V T A. **Influence of temperature and porosities on free vibration of a three-phase bidirectional functionally graded sandwich beam**. *Sci. Tech. Dev. J. – Engineering and Technology* 2023; 5(SI2): 65-76.

All references discussed in the above paragraph, however deal with the beams with the material properties varying in the thickness direction only. It is of great demand of practice to have FGM structures whose material properties change more directions for withstand the complex multi-directional loading. To the author's best knowledge, investigation on the effect of temperature rise on the vibration of three-phase porous FGSW beams has not been reported until now. As an attempt to narrow this gap, this paper presents a free vibration analysis of a porous sandwich beam made of three-phase composite material (BFGSW beam) in a temperature environment for the first time. The analysis is performed in the framework of a hyperbolic shear deformation theory [14]. The beam considered herein is composed of a homogeneous core layer and two face layers made of three-phase composite with effective properties varying in both the length and thickness by power-law functions. Employing the finite element method, the discretized equation of motion is established and solved for natural frequencies. Numerical study is presented to show the validation of the proposed formulation. The effects of various factors such as the porosities, temperature rise, power-lă indicies and the beam geometry on the vibration bahaviour of the sandwich beam are investigated in detail and discussed.

METHOD

Porous BFGSW beam

Figure 1 illustrates a porous BFGSW beam with simply supported ends and rectangular cross section (bxh). The beam formed from three layers, a homogenous core and two face layers made from three-phase composite with material properties varying in both the longitudinal and thickness directions. The Cartersian coordinate system (x,y,z) is chosen as well as its plane (x-y) is coincident with the mid-plane. Denoting in the figure, z_0=-h/2, z_1, z_2 and z_3=h/2 are the vertical coordinates measured from the mid-plane of the bottommost surface, the interface faces between the layers and the topmost surface, respectively.

The beam material is considered herein to be formed from three distinct materials, M_1, M_2 and M_3, whose volume fraction is expressed as Nguyen [15].

$$\begin{cases} V_1 = \left(\frac{z-z_0}{z_1-z_0}\right)^{n_s} \\ V_2 = \left[1-\left(\frac{z-z_0}{z_1-z_0}\right)^{n_s}\right]\left[1-\left(\frac{x}{L}\right)^{n_x}\right],\ z\in[z_0,z_1] \\ V_3 = \left[1-\left(\frac{z-z_0}{z_1-z_0}\right)^{n_s}\right]\left(\frac{x}{L}\right)^{n_x} \end{cases}$$
$$V_1 = 1,\ V_2 = V_3 = 0\ for\, z\in[z_1,z_2]$$
$$\begin{cases} V_1 = \left(\frac{z-z_3}{z_2-z_3}\right)^{n_s} \\ V_2 = \left[1-\left(\frac{z-z_3}{z_2-z_3}\right)^{n_s}\right]\left[1-\left(\frac{x}{L}\right)^{n_x}\right],\ z\in[z_2,z_3] \\ V_3 = \left[1-\left(\frac{z-z_3}{z_2-z_3}\right)^{n_s}\right]\left(\frac{x}{L}\right)^{n_x} \end{cases} \quad (1)$$

where V_1, V_2 and V_3 respectively denotes the volume fraction of the materials M_1, M_2 and M_3; n_x and n_z are the length and thickness material indexes; L is the total beam length.

The properties of constituent materials are assumed in the present paper are changed by temperature. In this regard, a typical material property P^i (i=1,2,3) varies with environment temperature T according to [10]

$$P^i(T) = P_0\left(P_{-1}T^{-1} + 1 + P_1T + P_2T^2 + P_3T^3\right) \quad (2)$$

In the above equation, P_{-1}, P_0, P_1, P_2, P_3 denote the temperature coefficients, and they are unique to each constituent material; $T = T_0 + \triangle T$, in which T_0=300 K is the reference temperature, while ΔT is the rise of temperature. In this paper, the temperature is considered uniformly rised in the beam.

Using the rule of mixture (alss known as the Voigt's model), an effective material properties, P_f, such as elastic modulus E_f, mass density ρ_f, Poisson's ratio υ_f, thermal expansion coefficient α_f with even porosity distribution are given by

$$P_f(x,z,T) = \begin{cases} \sum_{i=1}^{3} P^i\left(V_i - \frac{a}{2}\right)\ for\ two\ surface layers \\ P^1\ for\ core layer \end{cases} \quad (3)$$

where P^i (i=1,2,3) is the material property of M_i; a (a << 1) [9] is the porosity volume fraction. In case a=0, the considered beam becomes is perfect, without any porosities.

Governing equations

According to the hyperbolic shear deformation theory [14], displacements of an arbitrary point in the beam in x and z directions, $u_1(x,z,t)$ and $u_3(x,z,t)$, respectively, are given by

$$\begin{aligned} u_1(x,z,t) &= u(x,t) - zw_{,x}(x,t) + f(z)\,\theta(x,t), \\ u_3(x,z,t) &= w(x,t) \end{aligned} \quad (4)$$

where $u(x,t)$ and $w(x,t)$ respectively denote displacements in x and z directions of the point on the (x,z)

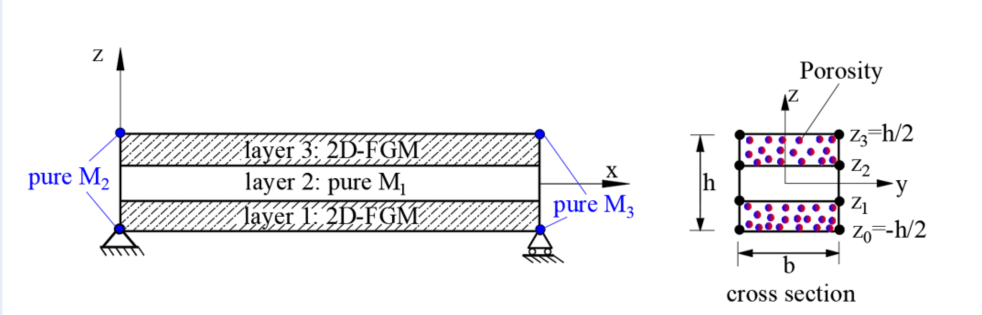

Figure 1: A simply supported porous BFGSW beam model

plane; $\theta(x,t)$ is the cross-sectional rotation, while t denote the variable of time. A subscript comma in Eq. (4) and in the below is used to indicate the derivative with respect to the variable that follows; the shape function $f(z)$ has the form

$$f(z) = z\cos h\left(\frac{1}{2}\right) - h\sin h\left(\frac{z}{h}\right) \quad (5)$$

The normal axial strain (ε_{xx}), and the shear strain (γ_{xs}) calculated from Eq. (4) are as follows

$$\begin{aligned}\varepsilon_{xx} &= u_{,x} - zw_{,xx} + f\theta_{,x},\\ \gamma_{xs} &= f_{,s}\theta\end{aligned} \quad (6)$$

Assuming a linear elastic behavior for the beam material, the relation between the stresses with the strains are given by

$$\begin{aligned}\sigma_{xx} &= E_f(x,z,T)\,\varepsilon_{xx},\\ \tau_{xs} &= G_f(x,z,T)\,\gamma_{xs}\end{aligned} \quad (7)$$

where σ_{xx} is the normal stress, τ_{xs} is the shear stress; $G_f(x,z,T) = \frac{E_f(x,z,T)}{2[1+\nu_f(x,z,T)]}$ is the effective shear modulus.

The elastic strain energy of the beam (U_B) is calculated as

$$U_B = \frac{1}{2}\int_0^L\int_A(\sigma_{xx}\varepsilon_{xx} + \tau_{xs}\gamma_{xs})\,dAdx \quad (8)$$

with A is the area of the beam cross section.

Using Eqs. (6) and (7), one can rewrite Eq. (8) in the following form

$$\begin{aligned}U_B = \frac{1}{2}\int_0^L&(A_{11}u_{,x}^2 - A_{12}u_{,x}w_{,xx}\\ &+A_{22}w_{,xx}^2 + 2A_{13}u_{,x}\theta_{,x} - 2A_{23}w_{,xx}\theta_{,x}\\ &+A_{33}\theta_{,x}^2 + B_{33}\theta^2)dx\end{aligned} \quad (9)$$

where the rigidities A_{11}, A_{12}, A_{22}, A_{13}, A_{23}, A_{33} and B_{33} are defined as follows

$$\begin{aligned}&(A_{11}, A_{12}, A_{22}, A_{13}, A_{23}, A_{33})\\ &= b\int_{z_0}^{z_3}E_f(x,z,T)\times\\ &\left[1, z, z^2, f(x), zf(z), f^2(z)\right]dz\\ &B_{33} = b\int_{z_0}^{z_3}G_f(x,z,T)\,f_{,z}^2(z)\,dz\end{aligned} \quad (10)$$

The strain energy due to the initial stresses by the temperature rise (U_T) is calculated as [2,4]

$$U_T = \frac{1}{2}\int_0^L N_T w_{,x}^2\,dx \quad (11)$$

where N_T denotes the thermal resultant, which can be calculated as

$$\begin{aligned}&N_T(x,z,T) =\\ &-b\int_{z_0}^{z_3}E_f(x,z,T)\,\alpha_f(x,z,T)\,\triangle T\,dz\end{aligned} \quad (12)$$

The kinetic energy (T) of the beam is given by

$$T = \frac{1}{2}\int_0^L\int_A\rho_f(x,z)\left(\dot{u}_1^2\dot{u}_3^2\right)dAdx \quad (13)$$

The over dot in the above equation and in the below denotes the derivative with respect to the variable t. From Eq. (4), one can recast the kinetic energy of the beam in the following form

$$\begin{aligned}T = \frac{1}{2}\int_0^L&[I_{11}\left(\dot{u}^2 + \dot{w}^2\right) - 2I_{12}\dot{u}\dot{w}_{,x}+\\ &I_{22}\dot{w}_{,x}^2 + 2I_{13}\dot{u}\dot{\theta} - 2I_{23}\dot{w}_{,x}\dot{\theta} + I_{33}\dot{\theta}^2]dx\end{aligned} \quad (14)$$

where I_{11}, I_{12}, I_{22}, I_{13}, I_{23}, I_{33} are the mass moments of the beam, which are defined as

$$\begin{aligned}&(I_{11}, I_{12}, I_{22}, I_{13}, I_{23}, I_{33})\\ &= b\int_{z_0}^{z_3}\rho_f(x,z)\times\\ &\left[1, z, z^2, f(z), zf(z), f^2(z)\right]dz\end{aligned} \quad (15)$$

Finite element formulation

Differential equations described th motion of the porous BFGSW beam in temperature environment can be derived by using Hamilton's principle for Eqs. (9), (11) and (14). However, due to the longitudinal variation of the beam properties, the rigidities, the thermal resultant and the mass moments, which can be seen from Eqs. (10), (12) and (15), are dependent on the axial coordinate x, and this causes difficulties in deriving an analytical solution for such differential equations. In this regard, the finite element method is employed herein to establish a discretized equation to describe motion of the beam.

Following the finite element analysis, the beam is considered herewith into a set of two-node beam elements with uniform length of l. The element has eight degrees of freedom, and the vector of nodal displacements (d) has the following form

$$d = \left\{ d_u \quad d_w \quad d_\theta \right\}^T \tag{16}$$

where

$$\begin{aligned} d_u &= \left\{ u_1 \quad u_2 \right\}^T, \; d_\theta = \left\{ \theta_1 \quad \theta_2 \right\}^T, \\ d_w &= \left\{ w_1 \quad w_{,x1} \quad w_2 \quad w_{,x2} \right\}^T \end{aligned} \tag{17}$$

are, respectively, the nodal displacement vectors of the u, w and θ. The superscript 'T' in above equations and in the below is used to indicate the transpose of a matrix or a vector.

The displacements and rotation inside the element are needed to interpolate from their nodal values as

$$u = N d_u, \; w = H d_w, \; \theta = N d_\theta \tag{18}$$

with N = $[N_1 N_2]$ and H = $[H_1 H_2 H_3 \; H_4]$ denote the interpolating function matrices of interpolation functions. In the present work, the functions N_i (i=1,2) and H_j (j=1÷4) are chosen as linear and cubic Hermite polynomials, respectively[15].

Using the interpolations, the strain energy (U_B) of the beam can be written in the following matrix form

$$U_B = \frac{1}{2} \overset{nel}{\Sigma} d^T k_B d \tag{19}$$

in which *nel* is the number of elements necessary to used for discreting the beam; k_B is the stiffness matrix of the element, and it can be written in submatrices as

$$\underset{8\times 8}{k_B} = \begin{bmatrix} k^B_{uu} & k^B_{uw} & k^B_{u\theta} \\ \left(k^B_{uw}\right)^T & k^B_{ww} & k^B_{w\theta} \\ \left(k^B_{u\theta}\right)^T & \left(k^B_{w\theta}\right)^T & k^B_{\theta\theta} \end{bmatrix} \tag{20}$$

In Eq. (20), k^B_{uu}, k^B_{ww}, $k^B_{\theta\theta}$, k^B_{uw}, k^B_{uu}, $k^B_{u\theta}$, $k^B_{w\theta}$ are the element stiffness matrices due to from the axial stretching, bending, shear, axial-bending coupling, axial-shear coupling and bending-shear coupling deformation, respectively. These matrices have the following forms

$$\begin{aligned} k^B_{uu} &= \textstyle\int_0^l N^T_{,x} A_{11} N_{,x} dx, \\ k^B_{ww} &= \textstyle\int_0^l H^T_{,xx} A_{22} H_{,xx} dx, \\ k^B_{\theta} &= \textstyle\int_0^l \left(N^T_{,x} A_{33} N_{,x} + N^T B_{33} N \right) dx, \\ k^B_{uw} &= -\textstyle\int_0^l N^T_{,xx} A_{12} H_{,xx} dx, \\ k^B_{u\theta} &= \textstyle\int_0^l N^T_{,x} A_{13} N_{,x} dx, \\ k^B_{w\theta} &= \textstyle\int_0^l H^T_{,xx} A_{23} N_{,x} dx \end{aligned} \tag{21}$$

The energy (U_T) due to the thermal effect in Eq. (11) can also be written in a matrix form as

$$U_T = \frac{1}{2} \overset{nel}{\Sigma} d^T k_T d \tag{22}$$

with $\underset{8\times 8}{k_T} = \begin{bmatrix} 0 & 0 & 0 \\ 0 & k_{TT} & 0 \\ 0 & 0 & 0 \end{bmatrix}$ where $\underset{4\times 4}{k_{TT}} = \int_0^l H^T_{,x} N_T H_{,x} dx$.

Thus, the total stiffness of the element is

$$k = k_B + k_T \tag{23}$$

The matrix form for the kinetic energy is as follows

$$T = \frac{1}{2} \overset{nel}{\Sigma} \dot{d}^T m \dot{d} \tag{24}$$

where m is the mass matrix of the element, and it can be written in sub-matrices as follows

$$\begin{aligned} m_{uu} &= \textstyle\int_0^l N^T I_{11} N dx, \\ m_{\theta\theta} &= \textstyle\int_0^l N^T I_{33} N dx, \\ m_{ww} &= \textstyle\int_0^l \left(H^T I_{11} H + H^T_{,x} I_{22} H_{,x} \right) dx, \\ m_{uw} &= -\textstyle\int_0^l N^T I_{12} H_{,x} dx, \\ m_{u\theta} &= \textstyle\int_0^l N^T I_{13} N dx, \\ m_{w\theta} &= -\textstyle\int_0^l H^T_{,x} I_{23} N dx \end{aligned} \tag{26}$$

Having the stiffness and mass matrices of the element derived, one can establissh the discretized equation of motion for the free vibration analysis of the beam with the following form

$$M\ddot{D} + KD = 0 \tag{27}$$

In the above equation, D is structural vector of nodal displacements M and K are the global mass and stiffness matrices resulted from the assembly of the element mass matrix m and stiffness matrix k over all the elements, respectively. To determine the frequency ω we asume a harmonic form for the vector of the nodal displacements in Eq. (27), and this lead to the eigenvalue problem of form

$$\left(K - \omega^2 M \right) \bar{D} = 0 \tag{28}$$

where $\bar{D}$ stand for the vibration amplitude. The standard method for an eigenvalue problem can be applied to sole Eq. (28).

RESULTS AND DISCUSSIONS

This section presents numerical investigations to highlight the influence of various factors such as the beam material and geometry parameters, the porosities and the temperature rise on the free vibration of the BFGSW beam with simply-supported ends. For this end, a beam is considered to be made from alumina (Al_2O_3) as M_1, zirconia (ZrO_2) as M_2 and steel

(SUS304) as M_3 with their material properties are given in Table 1 [11,16]. The geometric data h=1 m, b=0.5 m are used in the computations.

The frequency parameters, μ_i, used in this paper are introduced as follows

$$\mu_i = \omega_i \frac{L^2}{h} \sqrt{\frac{\rho_{SUS304}}{E_{SUS304}}} \tag{29}$$

where ω_i is the ith natural frequency. In order to study the effect of the beam thickness ratio, three numbers in brackets, e.g. (2-1-2) stands for that the thickness ratio of the bottom, core and top layers is adopted herein.

The proposed formulation is firstly verified before computing the vibration characteristics. For this purpose, in Table 2, the frequency parameters of a BFGSW.

beam with a ration of length-to-height, L/h=20, without the influence of temperature obtained in the this work are compared with the result in Ref. [15] using the sinusoidal beam theory and an enriched beam element. One can see from Table 2 a good agreement between the frequency parameters of in this paper with the ones of Ref. [15]. Furthermore, the fundamental frequency parameters of porous FG beam in the temperature environment calculated in this paper are compared with the results based on Euler-Bernoulli beam theory and the Navier type method of Ebrahimi et al. [11] in Table 3 for different porosity parameter and thermal loading. It is gain observed the good agreement between the two results from Table 3.

The convergence of the proposed beam element in calculating the vibration frequencies of the porous BFGSW beam in a temperature environment is shown in Table 4. In this table, the frequencies of (1-2-1) and (2-2-1) beams are calculated for L/h=20, a=0.1, ΔT=20 K and various power-law indexes nx and nz. As seen in Table 4, convergence is achieved by using eighteen elements derived herein, irrespective of the power-law indexes.

The effect of temperature rise and grading indexes on the first frequency parameter of porous BFGSW beam with a=0.1, L/h=20, various layer thickness ratios is presented in Table 5. The table shows that an increase in the transverse index nz results in a decrease in frequency parameters, regardless of the temperature rise, axial poer-law index and the ratio of layer thickness. It is easy to observe from Table 5 that rise of temperature and the ratio of layer thickness have a signification effect on the frequency parameter. The first frequency parameter is smaller for the beam associated with a lower core thickness and a higher value of the temperature rise, regardless of the power-law indexes.

The dependence of frequency parameter μ_1 on the temperature rise and the grading indexes is also depicted in Figure 2 for the (1-2-2) beam. As observed from Figure 2 and Table 5, the increase in temperature rise affects the dependence of μ_1 on the axial grading index n_x. With low temperature rise, the frequency parameter increases by increasing the axial grading index n_x, on the contrary, this rule is incorrect.

The variation of the first four frequency parameters of (1-2-2) beam with the power-law indexes is illustrated in Figure 3 for L/h=10, a=0.1, ΔT=20 K. It can be seen from the figure that the higher frequency parameters have similar relation with the power-law indexes as the first frequency parameter does. All the frequency parameters are increased when increase the thickness index n_x and they are decreased by increasing the index n_z.

The influence of the porosities on the relationship of the first frequency parameter μ_1 and the power-law indexes is shown in Figure 4 for (1-2-2) beam. Different porosity parameters are considered as a={0, 0.1, 0.2} along with L/h=10, ΔT=20 K. Figure 4a shows that increasing the value of porosity parameter leads to an increase in the frequency parameter with the transverse power-law index n_z in the range from 0 to 0.6, and a decrease in the parameter μ_1 with the decrease of the index n_z in the range from 0.6 to 5. Meanwhile, as seen from Figure 4b, the parameter μ_1 increases by increasing the porosity parameter, regardless of the axial grading index n_x.

Figure 5 and Figure 6 show the variation of the first frequency parameter μ_1 of BFGSW beams with temperature rise for different power-law indexes and the porosity parameters, respectively. As can be observed from these figures, the first frequency parameter decreases by increasing the rise of temperature, irrespective of the power-law indexes, the porosity parameter and the beam layer thickness ratio. However, for the case of asymmetric beam, Figure 6b, this only occurs for a temperature rise larger than 25 K.

The effect of the length-to-height ratio on the first frequency parameter of (1-2-2) beam can see from Figure 7, where the variation of the first frequency parameter with the length-to-height ratio is shown for different porosities, Figure 7a, and different temperature rises, Figure 7b. In the case of ΔT=0, as seen from Figure 7a, the parameter μ_1 increases when increase of the length-to-height ratio, regardless of the porosity parameter. The rise of temperature has an impact effect on the shape of the frequency parameter- temperature rise curves, as can be seen from Figure 7b. The first frequency parameter firstly increases, and it then decreases when increase value of the length-to-height ratio L/h.

Table 1: Temperature dependent coefficients of Young's modulus E, mass density ρ, Poisson's ratio ν, thermal expansion α for constituent materials of the BFGSW beam

Properties	Material	P_0	P_{-1}	P_1	P2	P3
E (Pa)	Al_2O_3	349.55x10^9	0	-3.853x10^{-4}	4.027x10^{-7}	1.673x10^{-10}
	SUS304	201.04x10^9	0	3.079x10^{-4}	-6.534x10^{-7}	0
	ZrO_2	132.2x10^9	0	-3.805x10^{-4}	-6.127x10^{-8}	0
ρ (kg/m^3)	Al_2O_3	3800	0	0	0	0
	SUS304	8166	0	0	0	0
	ZrO_2	3657	0	0	0	0
ν	Al_2O_3	0.26	0	0	0	0
	SUS304	0.3262	0	-2.002x10^{-4}	3.797x10^{-7}	0
	ZrO_2	0.3330	0	0	0	0
α (K^{-1})	Al_2O_3	6.8269x10^{-6}	0	1.838x10^{-4}	0	0
	SUS_304	12.330x10^{-6}	0	8.086x10^{-4}	0	0
	ZrO_2	13.300x10^{-6}	0	-1.421x10^{-3}	9.549x10^{-7}	0

Table 2: Comparison of the first frequency parameter of BFGSW beam for L/h=20 and different power-law indexes and layer thickness ratios (without thermal stresses)

n_x	n_z	1-0-1		2-1-2		2-1-1		2-2-1	
		Ref.15	Presen	Ref.15	Presen	Ref.15	Presen	Ref.15	Present
0.5	0.5	4.4296	4.4387	4.5289	4.5357	4.6033	4.6095	4.7067	4.7114
	1	3.9099	3.9098	4.0451	4.0450	4.1666	4.1666	4.3174	4.3175
	2	3.4644	3.4643	3.5960	3.5959	3.7675	3.7676	3.9472	3.9473
	5	3.2093	3.2091	3.2607	3.2606	3.4699	3.4700	3.6379	3.6381
1	0.5	4.4992	4.5076	4.5900	4.5963	4.6590	4.6648	4.7545	4.7589
	1	4.0258	4.0257	4.1461	4.1461	4.2578	4.2578	4.3949	4.3950
	2	3.6296	3.6295	3.7417	3.7416	3.8971	3.8972	4.0572	4.0573
	5	3.4123	3.4121	3.4474	3.4472	3.6343	3.6344	3.7797	3.7798
5	0.5	4.6481	4.6550	4.7210	4.7262	4.7788	4.7836	4.8574	4.8611
	1	4.2712	4.2711	4.3613	4.3612	4.4523	4.4523	4.5609	4.5609
	2	3.9756	3.9755	4.0489	4.0488	4.1713	4.1713	4.2913	4.2914
	5	3.8324	3.8322	3.8374	3.8373	3.9788	3.9789	4.0793	4.0794

CONCLUSIONS

The effects of the porosities and the rise of temperature on vibration characteristics of a three-phase BFGSW beam has been investigated in this paper in the framework of the hyperbolic shear deformation beam theory. The sandwich beam composed of an isotropic homogeneous core and two face layers of three-phase composite material. The material properties of the face layers are considered to vary in both the axial and transverse directions by the power-laws functions. A simple eight degrees of freedom finite element formulation was formulated and used to establish the discretized equation of motion for the beam. The accuracy and convergence of the proposed formulation have been validated by comparing the present results with the ones available in the literature. The numerical results obtained in the present work show that the temperature rise, the material dis-

Table 3: Comparison of the first frequency parameter of porous FG beam with different porosity parameter and thermal loading (n_x=0, L/h=20)

ΔT	a	n_z=0.1		n_z=0.2		n_z=0.5		n_z=1	
		Ref.11	Present	Ref.11	Present	Ref.11	Present	Ref.11	Present
20	0	4.6535	4.6462	4.3866	4.3853	3.8973	3.9020	3.5192	3.5292
	0.1	4.8339	4.8285	4.5215	4.5230	3.9597	3.9688	3.5345	3.5508
	0.2	5.0693	5.0665	4.6924	4.6978	4.0327	4.0479	3.5470	3.5718
40	0	4.4516	4.4388	4.1782	4.1719	3.6778	3.6786	3.2923	3.2996
	0.1	4.6575	4.6464	4.3385	4.3349	3.7657	3.7710	3.3334	3.3472
	0.2	4.9182	4.9095	4.5346	4.5347	3.8638	3.8752	3.3713	3.3938
80	0	4.0148	3.9894	3.7212	3.7037	3.1833	3.1763	2.7692	2.7722
	0.1	4.2828	4.2585	3.9442	3.9290	3.3361	3.3334	2.8776	2.8872
	0.2	4.6038	4.5809	4.2009	4.1886	3.4962	3.4994	2.9792	2.9979

Table 4: Convergence of the beam element in evaluating frequency of porous BFGSW beam with L/h=20, a=0.1, ΔT=20 K

Beam	n_x	n_z	nel=6	nel=8	nel=10	nel=12	nel=14	nel=16	nel=18
1-2-1	0.5	0.5	4.2525	4.2524	4.2523	4.2523	4.2523	4.2523	4.2523
		2	3.5804	3.5803	3.5803	3.5802	3.5802	3.5802	3.5802
		5	3.3146	3.3145	3.3145	3.3144	3.3144	3.3144	3.3144
	3	0.5	4.3125	4.3123	4.3123	4.3122	4.3122	4.3122	4.3122
		2	3.5926	3.5924	3.5924	3.5923	3.5923	3.5923	3.5923
		5	3.2872	3.2870	3.2870	3.2870	3.2870	3.2870	3.2870
2-2-1	0.5	0.5	4.1954	4.1951	4.1950	4.1950	4.1950	4.1950	4.1950
		2	3.4720	3.4716	3.4715	3.4714	3.4714	3.4713	3.4713
		5	3.2081	3.2077	3.2075	3.2074	3.2074	3.2073	3.2073
	3	0.5	4.2813	4.2810	4.2809	4.2809	4.2808	4.2808	4.2808
		2	3.5115	3.5108	3.5106	3.5104	3.5104	3.5103	3.5103
		5	3.2158	3.2150	3.2146	3.2145	3.2143	3.2143	3.2143

tribution and the beam geometry are important factors that significantly influence the natural frequencies of the BFGSW beam. Though the numerical investigations are carried out in the presented work for the beam with simply supported ends only, the formulation proposed herein can be used to study vibration of three-phase BFGSW beams with other types of boundary conditions as well.

ACKNOWLEDGEMENTS

This research is funded by University of Transport and Communications (UTC) under grant number T2023-CB-003.

CONFLICT OF INTEREST

There is no conflict of interest.

AUTHORS' CONTRIBUTION

Pham Thi Ba Lien: validation, formal analysis, writing draft.

Vu Thi An Ninh: software, review and editing.

REFERENCES

1. Ghatage PS, Kar VR, Sudhagar PE. On the numerical modelling and analysis of multi-directional functionally graded composite structures. A review, Composite Structures. 2020; 236: 111837;Available from: https://doi.org/10.1016/j.compstruct.2019.111837.

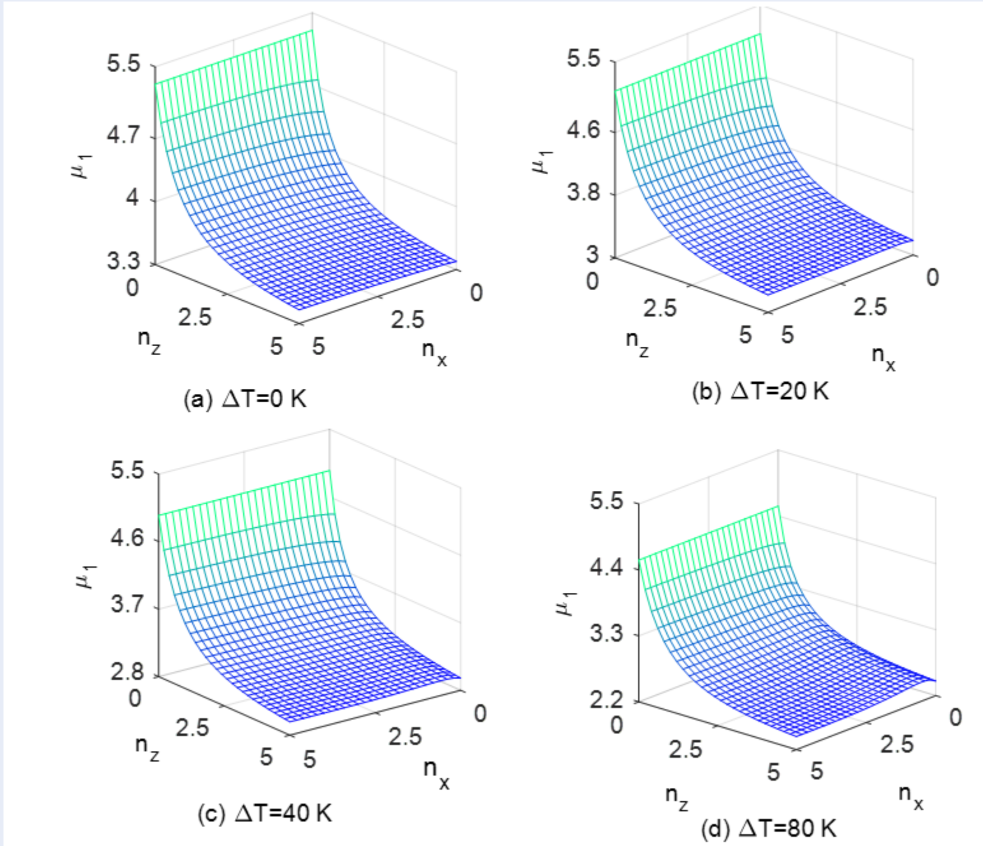

Figure 2: Variation of the first frequency parameter μ_1 of (1-2-2) beam with the power-law indexes for different temperature rise (L/h=20, a=0.1)

2. Mahi A, Bedia EA, Tounsi A, Mechab I. An analytical method for temperature-dependent free vibration analysis of functionally graded beams with general boundary conditions. Composite structures. 2010; 92: 1877-87;Available from: https://doi.org/10.1016/j.compstruct.2010.01.010.
3. Trinh LC, Vo TP, Thai HT, Nguyen TK. An analytical method for the vibration and buckling of functionally graded beams under mechanical and thermal loads. Composites Part B: Engineering. 2016; 100: 152-163;Available from: https://doi.org/10.1016/j.compositesb.2016.06.067.
4. Thom TT, Kien ND. Free vibration analysis of 2-D FGM beams in thermal environment based on a new third-order shear deformation theory. Vietnam Journal of Mechanics. 2018; 40: 121-40;Available from: https://doi.org/10.15625/0866-7136/10503.
5. Pradhan SC, Murmu T. Thermo-mechanical vibration of FGM sandwich beam under variable elastic foundations using differential quadrature method. Journal of Sound and Vibration. 2009; 321: 342-362;Available from: https://doi.org/10.1016/j.jsv.2008.09.018.
6. Setoodeh AR, Ghorbanzadeh M, Malekzadeh P. A two-dimensional free vibration analysis of functionally graded sandwich beams under thermal environment. Proceedings of the Institution of Mechanical Engineers, Part C: Journal of Mechanical Engineering Science. 2012; 226: 2860-2873;Available from: https://doi.org/10.1177/0954406212440669.
7. Tran TT, Nguyen NH, Do TV, Minh PV, Duc ND. Bending and thermal buckling of unsymmetric functionally graded sandwich beams in high-temperature environment based on a new third-order shear deformation theory. Journal of Sandwich Structures & Materials. 2021; 23: 906-930;Available from: https://doi.org/10.1177/1099636219849268.
8. Wattanasakulpong N, Ungbhakorn V. Linear and nonlinear vibration analysis of elastically restrained ends FGM beams with porosities. Aerospace Science and Technology. 2014; 32: 111-120;Available from: https://doi.org/10.1016/j.ast.2013.12.002.
9. Ait Atmane H, Tounsi A, Bernard F. Effect of thickness stretching and porosity on mechanical response of a functionally graded beams resting on elastic foundations. International Journal of Mechanics and Materials in Design. 2017; 13: 71-84;Available from: https://doi.org/10.1007/s10999-015-9318-x.
10. Akbaş ŞD. Thermal effects on the vibration of functionally graded deep beams with porosity. International Journal of Applied Mechanics. 2017; 9: 1750076;Available from: https://doi.org/10.1142/S1758825117500764.
11. Ebrahimi F, Ghasemi F, Salari E. Investigating thermal effects on vibration behavior of temperature-dependent compositionally graded Euler beams with porosities. Meccanica. 2016; 51: 223-249;Available from: https://doi.org/10.1007/s11012-015-0208-y.
12. Ebrahimi F, Jafari A. A four-variable refined shear-deformation beam theory for thermo-mechanical vibration analysis of temperature-dependent FGM beams with porosities. Mechanics of Advanced Materials and Structures. 2018; 25: 212-224;Available from: https://doi.org/10.1080/15376494.2016.1255820.
13. Liu Y, Su S, Huang H, Liang Y. Thermal-mechanical coupling buckling analysis of porous functionally graded sandwich

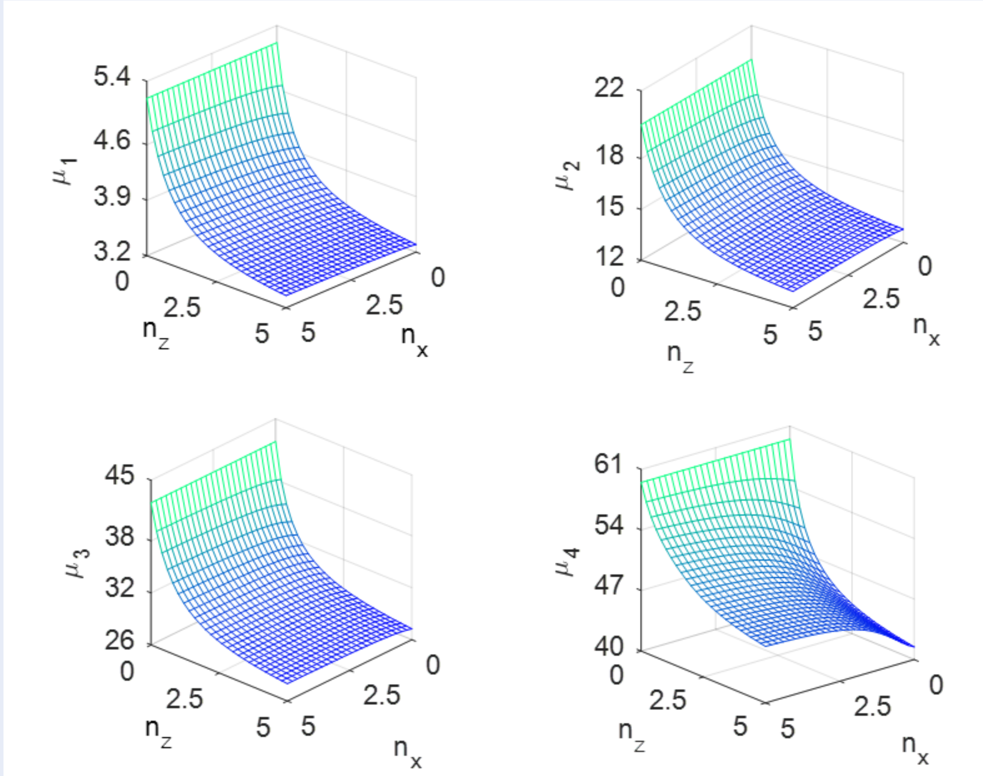

Figure 3: Variation of the first four frequency parameters of (1-2-2) beam with the power-law indexes for L/h=10, a=0.1, ΔT=20 K

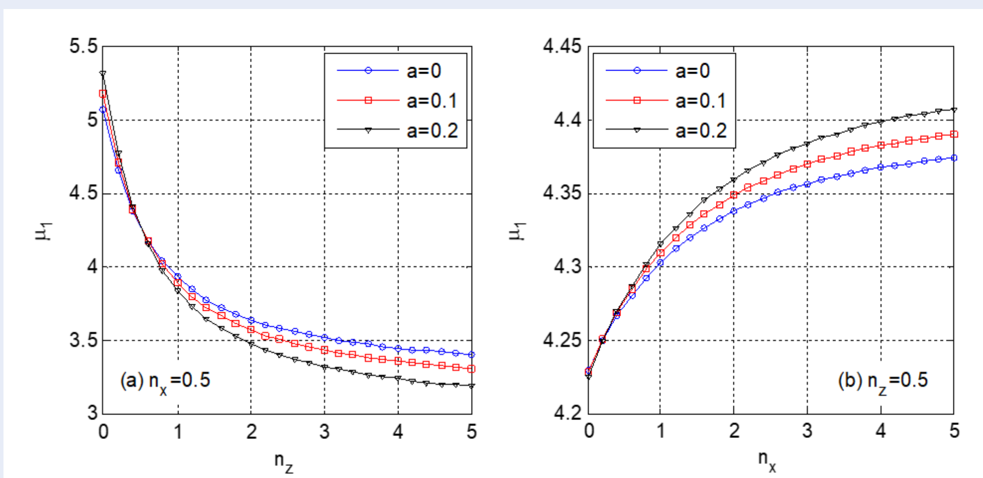

Figure 4: Variation of fundamental frequency parameters of (1-2-2) beam with the grading index for L/h=10, ΔT=20 K and different porosity parameters

Table 5: Fundamental frequency parameter of porous BFGSW beam with different temperature rise, grading indexes and layer thickness ratios (a=0.1, L/h=20)

ΔT	n_x	n_z	1-0-1	2-1-2	2-1-1	1-1-1	1-2-2	1-2-1	1-8-1
20	0.5	1	3.4044	3.5441	3.6401	3.6717	3.7931	3.8851	4.4595
		3	2.8678	3.0133	3.1380	3.1622	3.3228	3.4332	4.2232
		5	2.7559	2.8886	3.0169	3.0325	3.2002	3.3075	4.1491
	2	1	3.5055	3.6083	3.7162	3.7192	3.8483	3.9203	4.4808
		3	2.9128	3.0134	3.1692	3.1507	3.3384	3.4270	4.2420
		5	2.8013	2.8765	3.0401	3.0044	3.2048	3.2863	4.1660
40	0.5	1	3.2119	3.3421	3.4393	3.4652	3.5877	3.6759	4.2537
		3	2.6749	2.8063	2.9335	2.9488	3.1119	3.2166	4.0140
		5	2.5666	2.6827	2.8135	2.8187	2.9891	3.0895	3.9389
	2	1	3.3029	3.3940	3.5043	3.5004	3.6319	3.7004	4.2704
		3	2.7057	2.7851	2.9462	2.9148	3.1083	3.1908	4.0248
		5	2.5990	2.6476	2.8169	2.7652	2.9721	3.0456	3.9466
80	0.5	1	2.7825	2.8917	2.9936	3.0061	3.1332	3.2137	3.8078
		3	2.2335	2.3318	2.4689	2.4614	2.6350	2.7277	3.5569
		5	2.1318	2.2076	2.3490	2.3269	2.5088	2.5939	3.4786
	2	1	2.8583	2.9205	3.0382	3.0168	3.1561	3.2164	3.8151
		3	2.2391	2.2628	2.4421	2.3751	2.5886	2.6565	3.5507
		5	2.1427	2.1198	2.3091	2.2121	2.4423	2.4958	3.4663

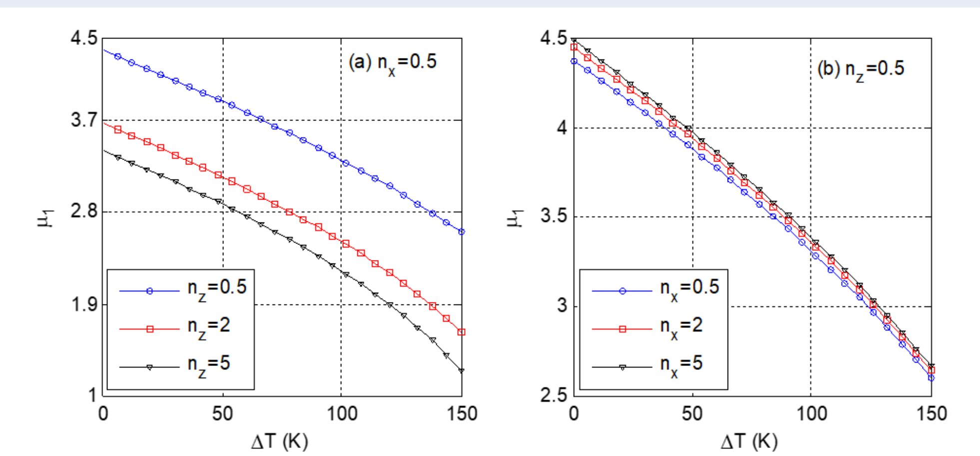

Figure 5: Variation of first frequency parameter of (1-2-2) beam with temperature rise for L/h=20, a=0.1: (a) n_x=0.5 and index n_z is variable; (b) n_z=0.5 and index is n_x variable

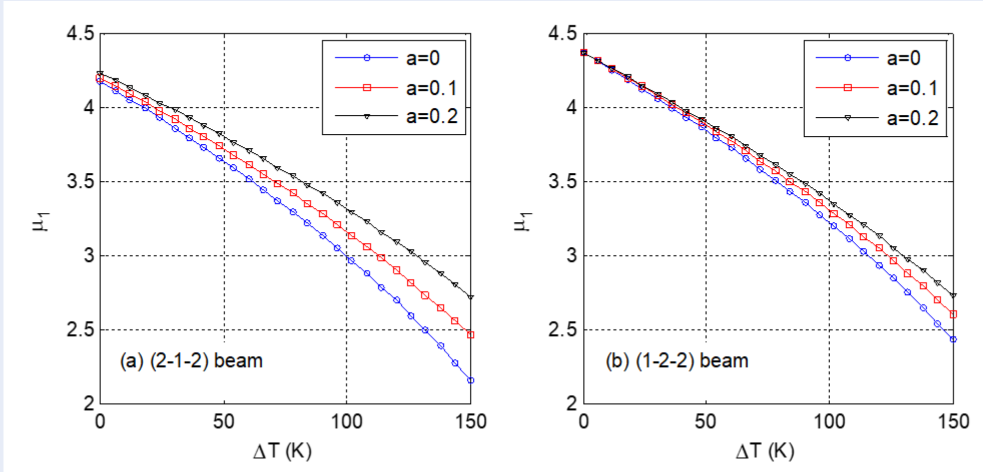

Figure 6: Variation of first frequency parameter with temperature rise for L/h=20, n_x=n_z=0.5 and different porosity parameters

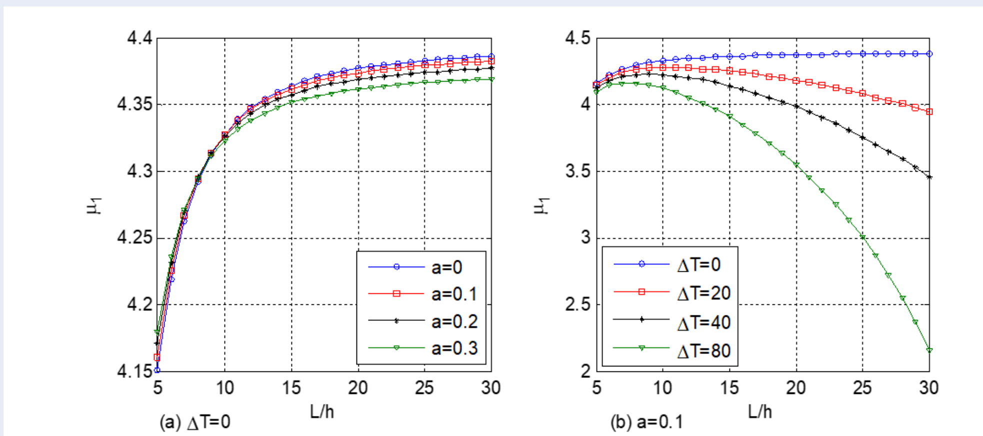

Figure 7: Variation of first frequency parameter of (1-2-2) beam with length-to-height ratio L/h for n_x=n_z=0.5: (a) ΔT=0 and different porosity parameters; (b) a=0.1 and different temperature rises

beams based on physical neutral plane. Composites Part B: Engineering. 2019; 168: 236-42;Available from: https://doi.org/10.1016/j.compositesb.2018.12.063.

14. Soldatos K. A transverse shear deformation theory for homogeneous monoclinic plates. Acta Mechanica.1992; 94: 195-220;Available from: https://doi.org/10.1007/BF01176650.

15. Nguyen DK, Vu ANT, Pham VN, Truong TT. Vibration of a three-phase bidirectional functionally graded sandwich beam carrying a moving mass using an enriched beam element. Engineering with Computers. 202; 1-22;.

16. Kim YW. Temperature dependent vibration analysis of functionally graded rectangular plates. Journal of sound and vibration. 2005; 284: 531-549;Available from: https://doi.org/10.1016/j.jsv.2004.06.043.

Tạp chí Phát triển Khoa học và Công nghệ – Engineering and Technology 2023, 5(SI2): 65-76
Open Access Full Text Article

Bài nghiên cứu

Ảnh hưởng của nhiệt độ và lỗ rỗng lên dao động tự do của dầm sandwich ba pha có cơ tính biến thiên hai chiều

Pham Thi Ba Lien, Vu Thi An Ninh*

TÓM TẮT
Sự hiểu biết về ảnh hưởng của một số yếu tố thực tế đến tần số riêng của dầm đóng vai trò quan trọng trong thiết kế loại kết cấu này. Ảnh hưởng của nhiệt độ và lỗ rỗng vi mô tới dao động tự do của dầm sandwich ba pha có cơ tính biến thiên hai chiều (BFGSW) được nghiên cứu lần đầu tiên trong bài báo này. Dầm sandwich gồm lõi thuần nhất và hai lớp mặt làm từ vật liệu composite ba pha. Các tính chất của vật liệu lớp mặt biến đổi liên tục theo cả chiều dài và chiều cao dầm theo hàm số mũ và chúng được đánh giá bằng mô hình Voigt. Tải nhiệt tăng đều và sự phân bố lỗ rỗng vi mô là đều cũng được xét đến. Năng lượng biến dạng, động năng của dầm cũng như năng lượng do nhiệt độ gây ra đã được xây dựng dựa trên lý thuyết biến dạng trượt hyperbolic. Phần tử dầm hai nút với tám bậc tự do đã được xây dựng và sử dụng để thiết lập phương trình chuyển động dạng rời rạc cho dầm. Độ chính xác của phương pháp đề xuất được khẳng bằng cách so sánh tham số tần số cơ bản với các tài liệu trước đó. Dầm với biên tựa hai đầu đã được sử dụng trong nghiên cứu số. Sự hội tụ của phần tử dầm cũng được đánh giá trên tần số cơ bản. Ảnh hưởng của sự tăng nhiệt độ, tỷ phần thể tích lỗ rỗng, chỉ số vật liệu, tỷ số chiều dài và chiều dày cũng như tỷ số độ dày các lớp dầm lên đặc trưng dao động đã được nghiên cứu và thảo luận chi tiết. Tóm lại, các tham số của dầm BFGSW, tham số lỗ rỗng và sự tăng nhiệt độ đóng vai trò quan trọng đối với tần số của dầm, và sự hiểu biết này giúp ta thiết kế các kết cấu dạng dầm với tần số mong muốn.
Từ khoá: Dầm BFGSW ba pha, lý thuyết hyperbolic, lỗ rỗng, tần số dao động, phương pháp phần tử hữu hạn

Trường Đại học Giao thông Vận tải, số 3 Cầu Giấy, Hà Nội, Việt Nam

Liên hệ

Vu Thi An Ninh, Trường Đại học Giao thông Vận tải, số 3 Cầu Giấy, Hà Nội, Việt Nam

Email: vuthianninh@utc.edu.vn

Lịch sử
- Ngày nhận: 20-4-2023
- Ngày chấp nhận: 12-9-2023
- Ngày đăng: 31-12-2023

DOI : https://doi.org/10.32508/stdjet.v6iSI2.1095

Trích dẫn bài báo này: Lien P T B, Ninh V T A. **Ảnh hưởng của nhiệt độ và lỗ rỗng lên dao động tự do của dầm sandwich ba pha có cơ tính biến thiên hai chiều**. *Sci. Tech. Dev. J. - Eng. Tech.* 2023, 5(SI2): 65-76.